

Role of magnetic ions in the thermal Hall effect of the paramagnetic insulator TmVO_4

Ashvini Vallipuram^{*,†}, Lu Chen^{*,‡}, Emma Campillo,¹ Manel Mezidi,^{1,2} Gaël Grissonnanche,^{3,4} Mark P. Zic,⁵ Yuntian Li,⁶ Ian R. Fisher,⁶ Jordan Baglo,¹ and Louis Taillefer^{1,7,§}

¹*Institut quantique, Département de physique & RQMP,
Université de Sherbrooke, Sherbrooke, Québec J1K 2R1 Canada*

²*Université Paris-Cité, Laboratoire Matériaux et Phénomènes Quantiques, CNRS (UMR 7162), 75013 Paris, France*

³*Laboratory of Atomic and Solid State Physics, Cornell University, Ithaca, NY 14853, USA*

⁴*Kavli Institute at Cornell for Nanoscale Science, Ithaca, NY 14853, USA*

⁵*Geballe Laboratory for Advanced Materials and Department of Physics, Stanford University, CA 94305, USA*

⁶*Geballe Laboratory for Advanced Materials and Department of Applied Physics, Stanford University, CA 94305, USA*

⁷*Canadian Institute for Advanced Research, Toronto, Ontario M5G 1M1, Canada*

(Dated: October 27, 2023)

In a growing number of materials, phonons have been found to generate a thermal Hall effect, but the underlying mechanism remains unclear. Inspired by previous studies that revealed the importance of Tb^{3+} ions in generating the thermal Hall effect of $\text{Tb}_2\text{Ti}_2\text{O}_7$, we investigated the role of Tm^{3+} ions in TmVO_4 , a paramagnetic insulator with a different crystal structure. We observe a negative thermal Hall conductivity in TmVO_4 with a magnitude such that the Hall angle, $|\kappa_{xy}/\kappa_{xx}|$, is approximately 1×10^{-3} at $H = 15$ T and $T = 20$ K, typical for a phonon-generated thermal Hall effect. In contrast to the negligible κ_{xy} found in $\text{Y}_2\text{Ti}_2\text{O}_7$, we observe a negative κ_{xy} in YVO_4 with a Hall angle of magnitude comparable to that of TmVO_4 . This shows that the Tm^{3+} ions are not essential for the thermal Hall effect in this family of materials. Interestingly, at an intermediate Y concentration of 30 % in $\text{Tm}_{1-x}\text{Y}_x\text{VO}_4$, κ_{xy} was found to have a positive sign, pointing to the possible importance of impurities in the thermal Hall effect of phonons.

I. INTRODUCTION

In the last decade, a thermal Hall effect has been measured in a number of insulators where phonons are the main heat carriers, including multiferroics such as $\text{Fe}_2\text{Mo}_3\text{O}_8$ [1], cuprates such as La_2CuO_4 [2, 3] and Nd_2CuO_4 [4], non-magnetic SrTiO_3 [5] and the antiferromagnet Cu_3TeO_6 [6]. In $\text{Tb}_3\text{Ga}_5\text{O}_{12}$ [7], the first insulator in which a thermal Hall signal was detected, the effect was attributed to skew scattering of phonons by superstoichiometric Tb^{+3} impurities [8].

Since then, a number of theoretical scenarios have been proposed to explain the origin of the phonon thermal Hall effect. Some attribute the thermal Hall conductivity κ_{xy} to the Berry curvature of phonon bands [9]. Others link it to various types of spin-lattice coupling [10–13]. In yet others, the role of impurities is considered important [14–16]. But it remains unclear which of these scenarios applies to what material.

In a previous study on pyrochlores [17], a sizeable κ_{xy} was observed in $\text{Tb}_2\text{Ti}_2\text{O}_7$ but a negligible κ_{xy} was detected in $\text{Y}_2\text{Ti}_2\text{O}_7$ (Fig. 1(b)). Although the κ_{xy} signal in $\text{Tb}_2\text{Ti}_2\text{O}_7$ was originally attributed to some exotic neutral excitations linked to the spin-liquid nature of the system [17], it was later argued that phonons are in fact responsible for the thermal Hall effect in this material [18], since a κ_{xy} signal of comparable magnitude is

still observed when 70% of the Tb ions are replaced by Y ions, and the spin state of the system is profoundly altered. Irrespective of the underlying mechanism, this study does show that Tb ions are essential for generating a thermal Hall effect in these pyrochlores.

Here we report a similar study carried out on a different oxide, TmVO_4 , wherein we investigate what happens to the thermal Hall effect when we substitute the magnetic ion Tm for the non-magnetic ion Y.

The insulator TmVO_4 exhibits a rich set of phenomena at low temperatures. It undergoes a cooperative Jahn-Teller phase transition at $T = T_D \simeq 2$ K in zero field, and at $H = H_D \simeq 0.5$ T at $T = 0$ (for $H//c$) [20]. The ordered state consists of a simultaneous ferroquadrupole order of the local 4f electronic orbitals of each Tm atom, accompanied by a structural transition, by which the crystal structure goes from tetragonal at high temperatures (I41/amd spacegroup [21]) to orthorhombic at low temperatures [20–24]. However, no magnetically ordered state has been reported in TmVO_4 [20]. Our own study will focus on temperatures above T_D .

II. METHODS

A. Samples

The following three rare-earth vanadates were studied: TmVO_4 , YVO_4 and $\text{Tm}_{0.7}\text{Y}_{0.3}\text{VO}_4$. The samples were grown using a flux growth method [25, 26]. They are needle shaped with their long axis along the c axis, which is the easy axis of magnetization [27]. Because TmVO_4 has a large anisotropy in its g -factor ($g_c = 10$ & $g_a = g_b =$

[†] * A.V. and L.C. contributed equally to this work.; ashvini.vallipuram@usherbrooke.ca

[‡] lu.chen@usherbrooke.ca

[§] louis.taillefer@usherbrooke.ca

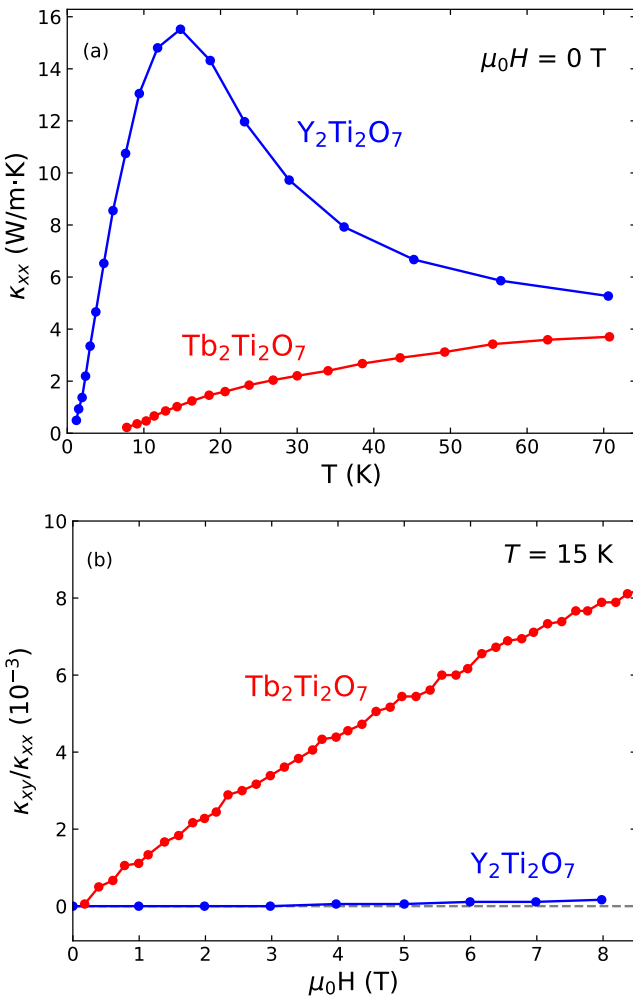


FIG. 1. Thermal transport in the pyrochlores $\text{Tb}_2\text{Ti}_2\text{O}_7$ (red) and $\text{Y}_2\text{Ti}_2\text{O}_7$ (blue). (a) Thermal conductivity κ_{xx} as a function of temperature, in zero magnetic field (from [19]). Note the much smaller conductivity of $\text{Tb}_2\text{Ti}_2\text{O}_7$ at low temperature, reflecting the presence of an additional scattering process. (b) Thermal Hall conductivity κ_{xy} , plotted as the thermal Hall angle $|\kappa_{xy}/\kappa_{xx}|$ vs field, at $T = 15$ K (from [17]). The Hall conductivity κ_{xy} in $\text{Y}_2\text{Ti}_2\text{O}_7$ is negligible, suggesting that Tb ions are necessary to generate a thermal Hall signal in this family of materials.

0) [28], even a slight misalignment of the magnetic field can cause a large torque on the sample, which can become detached from its mount.

Two measures were adopted to prevent this. First, the thermal transport contacts on TmVO_4 and $\text{Tm}_{0.7}\text{Y}_{0.3}\text{VO}_4$ samples were made with silver epoxy to ensure strong contacts that would adhere to a very smooth surface and wouldn't peel off. These contacts were solidified for about 10 minutes on a hot plate at 150 °C. Note that the contacts on the YVO_4 samples were done with silver paint, since there is no magnetic torque in this case. For the heater contact, a 50 μm diameter silver wire was used and for the thermal transport contacts,

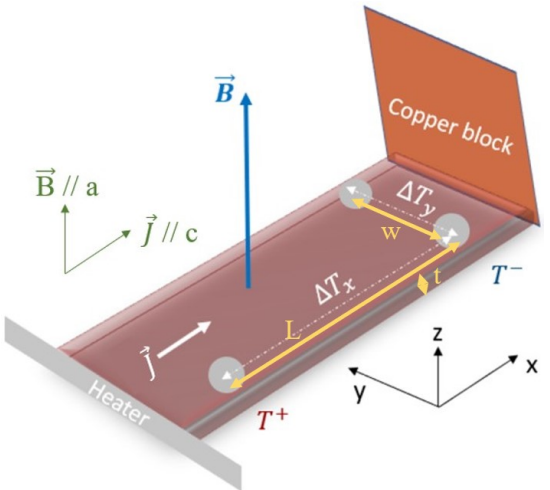


FIG. 2. Experimental setup used to measure κ_{xx} and κ_{xy} . A heat current J is generated along the x axis (c axis of the sample) and a magnetic field B is applied perpendicular to it, along the z axis (a axis of the sample). Differences in temperature are measured along the x axis (longitudinal temperature difference, ΔT_x) and the y axis (transverse temperature difference, ΔT_y).

wires with a diameter of 25 μm were used.

In addition, a small wood stick was positioned along the TmVO_4 and $\text{Tm}_{0.7}\text{Y}_{0.3}\text{VO}_4$ samples, and was linked to the sample by the heater wire. The thermal conductivity κ_{xx} was measured with and without the wood stick and only a 5 % (8 %) difference was observed (at the peak temperature) for TmVO_4 ($\text{Tm}_{0.7}\text{Y}_{0.3}\text{VO}_4$). The sample dimensions are given in Table I.

B. Thermal transport measurements

To perform a conventional thermal transport study, a 5-contact measurement is done using a steady-state method at a fixed field, as sketched in Fig. 2. A heat current (\vec{J}) is generated along the x axis from the heater contact on one end of the sample and the copper block on the other end. The heater was a strain gauge of 5 $\text{k}\Omega$ that has a resistance that does not change with temperature and field. This heat current was applied along the c axis of the sample (the x axis in Fig. 2), while the field B was applied along the a axis (the z axis in Fig. 2). Note that the field ($H = 0, 10$ and 15 T) was applied at high temperatures (at 83 K) and the samples were cooled down to $\simeq 3$ K using a variable temperature insert.

Temperature steps from $\simeq 3$ K to 80 K were done at fixed fields and all the temperature signals were stable before measuring each temperature difference (ΔT_x and ΔT_y in Fig. 2) using type-E (chromium/constantan) thermocouples. Note that for all the voltages, the background voltage (when the heat is off) is subtracted from the measured signal (when the heat is on).

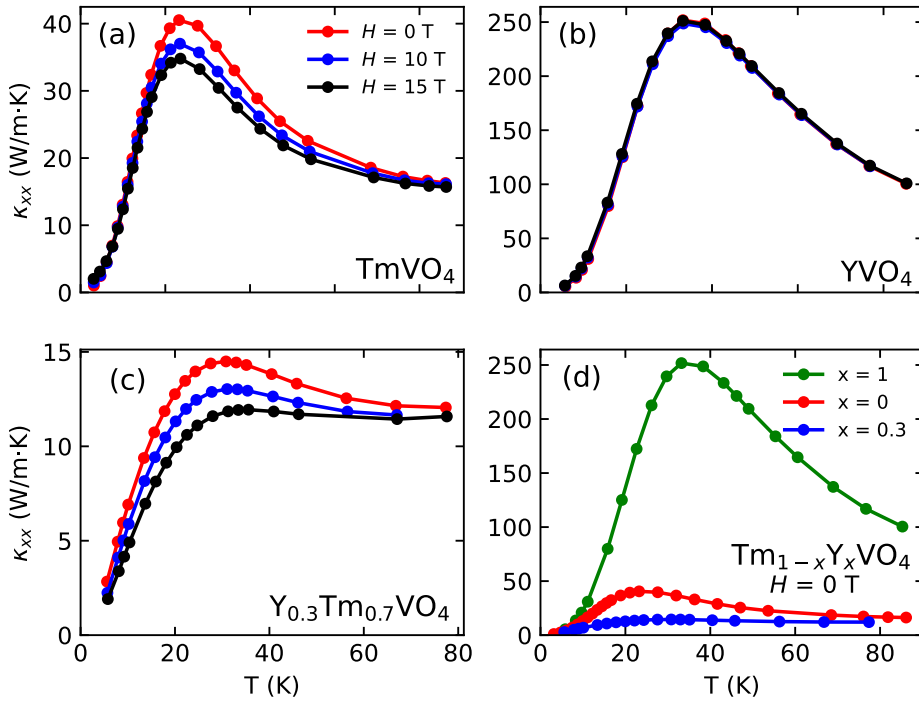


FIG. 3. Thermal conductivity of TmVO_4 (a), YVO_4 (b) and $\text{Y}_{0.3}\text{Tm}_{0.7}\text{VO}_4$ (c) as a function of temperature, measured with a heat current $J//c$ and a magnetic field $H//a$ ($H \perp J$, for $H = 0$ (red), 10 T (blue) and 15 T (black)). (d) Comparison of the three conductivities at $H = 0$. We see that substituting Y for Tm causes a major reduction in κ_{xx} , which is then further reduced if Y impurities are added.

The conductivities κ_{xx} and κ_{xy} were measured as described elsewhere [2–4].

Note that the transverse temperature difference ΔT_y is obtained by measuring in both field polarities ($+H$ and $-H$) and then antisymmetrizing the measured signals in order to get rid of any longitudinal contributions due to a possible slight misalignment of the transverse contacts:

$$\Delta T_y(H) = [\Delta T_y(T, H) - \Delta T_y(T, -H)]/2 \quad . \quad (1)$$

The thermal conductivity is defined as:

$$\kappa_{xx} = \frac{J}{\Delta T_x \cdot \alpha} \quad , \quad (2)$$

where J is the thermal current and α is a geometric factor ($\alpha = \frac{w \cdot t}{L}$; see Table I for sample dimensions). The thermal Hall conductivity is defined as:

$$\kappa_{xy} = \frac{\kappa_{yy} \cdot \Delta T_y \cdot L}{\Delta T_x \cdot w} \quad . \quad (3)$$

	L (mm)	w (mm)	t (mm)
TmVO_4	0.66	0.24	0.04
YVO_4	0.49	0.25	0.06
$\text{Y}_{0.3}\text{Tm}_{0.7}\text{VO}_4$	0.65	0.45	0.04

TABLE I. Dimensions of the three samples investigated here. L = length between contacts; w = width of the sample; t = thickness of the sample.

Note that here we assume that $\kappa_{yy} = \kappa_{xx}$ (i.e. that $\kappa_a = \kappa_c$), but this is not quite right since the c -axis conductivity is not identical to the a -axis conductivity. This implies that the amplitude of κ_{xy} reported here is not quite accurate, and would need to be multiplied by the anisotropy factor κ_a/κ_c . Given the needle shape of our samples, measurements with $J//a$ have not yet been done.

III. RESULTS

A. Thermal conductivity, κ_{xx}

The thermal conductivity κ_{xx} of our three samples is displayed in Fig. 3. All three curves are typical of insulators, with a peak near $T \simeq 20 - 30$ K. The zero-field curves are compared in Fig. 3(d), where we see that κ_{xx} in YVO_4 is much larger than in the other two. The magnitude of κ_{xx} in the stoichiometric sample of paramagnetic TmVO_4 is much lower presumably because phonons are scattered by spins. This is also presumed to be the case in the frustrated spin system $\text{Tb}_2\text{Ti}_2\text{O}_7$, except that here the scattering process is much stronger, resulting in a value of $\kappa_{xx} \simeq 2$ W/m·K at $T = 20$ K (Fig. 1(a)), compared to $\kappa_{xx} \simeq 40$ W/m·K in TmVO_4 (Fig. 3(a)).

As in the case of $\text{Tb}_2\text{Ti}_2\text{O}_7$, where the field dependence of κ_{xx} is exceptionally strong [19], we view the

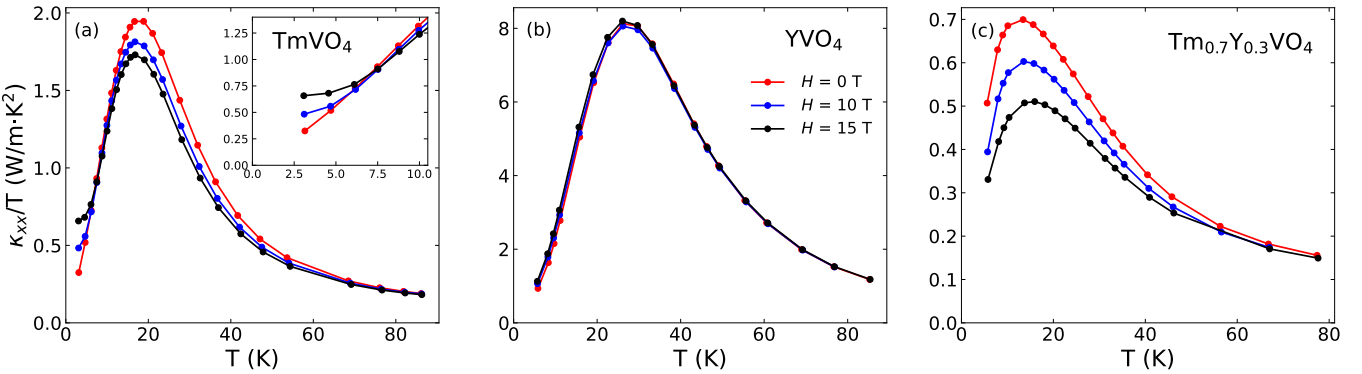


FIG. 4. Thermal conductivity of TmVO₄ (a), YVO₄ (b) and Tm_{0.7}Y_{0.3}VO₄ (c), for different applied magnetic fields, as indicated, plotted as κ_{xx}/T vs T to emphasize the low temperature regime. Note the strong field dependence in the two samples that contain Tm ions, compared to the much weaker field dependence in YVO₄. In panel (a), the inset shows a zoom below 10 K, where we see a different regime of H dependence, with a strong *increase* in κ_{xx} with increasing H .

sizable field dependence we observe in the conductivity of TmVO₄ (Fig. 3(a)), and Tm_{0.7}Y_{0.3}VO₄ (Fig. 3(c)), as a confirmation that phonons are scattered by spins associated with the Tm ions. The weaker field dependence seen in YVO₄ (Fig. 3(b)) is consistent with that picture. We attribute the fact that κ_{xx} in Tm_{0.7}Y_{0.3}VO₄ is even smaller than in TmVO₄ to the stronger disorder scattering of phonons in this more disordered system (Fig. 3(d)).

In Fig. 4, we plot κ_{xx}/T vs T , to emphasize the data at low temperature. We see that below 7 K or so, the field dependence of κ_{xx} in TmVO₄ becomes very strong and opposite in sign relative to its behaviour at higher temperature (inset of Fig. 4(a)). This change of regime is presumably associated with the approaching transition at T_D .

The thermal conductivity of TmVO₄ was measured previously [29]. These early measurements were done with $J//H//c$ (along the easy axis [27]) for $H < 7$ T and for $T < 30$ K, whereas our measurements were done with $J//c$ and $H//a$, covering a larger temperature and field range. This previous study reports a slightly higher κ_{xx} peak, perhaps due to a better sample quality. The field was seen to increase κ_{xx} at low temperatures ($T < 6$ K).

In our study, we also see an increase in κ_{xx} with H at low temperatures ($T < 8$ K; inset of Fig. 4a). However, we find that κ_{xx} decreases with H for $T > 10$ K or so (Fig. 4a). Interestingly, this change from increasing with H to decreasing with H as the temperature is raised above 10 K was actually captured by theoretical calculations that consider the main scattering of phonons to be the resonant scattering off electronic levels of the Tm ions [30, 31]. As the field increases, energy levels separate and the resonant conditions for scattering are satisfied for phonons of higher energy, thermally excited at higher temperatures. This resonant scattering off Tm ions is then presumably the reason why κ_{xx} in TmVO₄ is much lower than that in YVO₄ (Fig. 3).

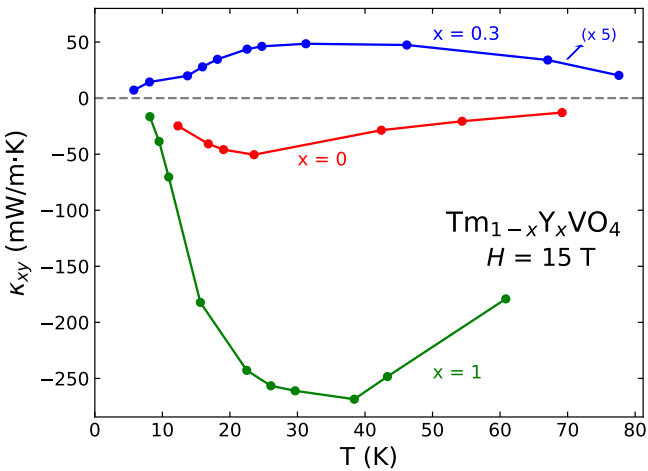


FIG. 5. Thermal Hall conductivity of TmVO₄ (red), YVO₄ (green) and Tm_{0.7}Y_{0.3}VO₄ (blue) as a function of temperature, measured with a heat current $J//c$ and a magnetic field $H//a$ ($H \perp J$), at $H = 15$ T. Note that κ_{xy} for Tm_{0.7}Y_{0.3}VO₄ has been multiplied by a factor of 5.

B. Thermal Hall conductivity, κ_{xy}

The thermal Hall conductivity κ_{xy} of our three samples is displayed in Fig. 5. Only data at $H = 15$ T are shown, but data at $H = 10$ T were also taken; they are similar but smaller in magnitude, roughly in proportion to the field amplitude. The first observation is that all three samples exhibit a non-negligible thermal Hall conductivity. The surprise is that the sign of κ_{xy} is negative in the two stoichiometric materials, TmVO₄ and YVO₄, but it is positive in the disordered sample Tm_{0.7}Y_{0.3}VO₄.

We see that the temperature at which $\kappa_{xy}(T)$ peaks (Fig. 5) is the same as the temperature at which the phonon-dominated $\kappa_{xx}(T)$ peaks (Fig. 3), for example $\simeq 25$ K in TmVO₄ and $\simeq 35$ K in YVO₄. As argued

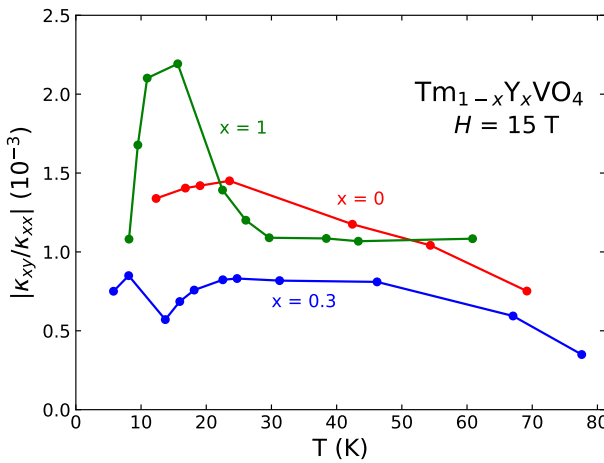


FIG. 6. Thermal Hall angle of TmVO_4 (red), YVO_4 (green) and $\text{Tm}_{0.7}\text{Y}_{0.3}\text{VO}_4$ (blue), plotted as $|\kappa_{xy}/\kappa_{xx}|$ vs T , for $H = 15$ T. At $T = 20$ K, the obtained value is around 1×10^{-3} for all three materials, a magnitude typical of the phonon Hall effect in several insulators [6, 32].

before for other materials [4–6, 32], this is an argument in support of phonons being the heat carriers responsible for the thermal Hall signal in these materials.

Looking at Fig. 5, we also notice that the magnitude of κ_{xy} appears to roughly scale with the magnitude of κ_{xx} seen in Fig. 3d. This is confirmed when looking at the thermal Hall angle, plotted as $|\kappa_{xy}/\kappa_{xx}|$ vs T in Fig. 6. Indeed, we see that $|\kappa_{xy}/\kappa_{xx}| \simeq 1 \times 10^{-3}$ at $T = 30$ K in both YVO_4 and $\text{Tm}_{0.7}\text{Y}_{0.3}\text{VO}_4$, even though the magnitude of κ_{xy} is 25 times larger in YVO_4 (Fig. 5). This is because κ_{xx} is also roughly 25 times larger in YVO_4 (Fig. 3).

IV. DISCUSSION

In the pyrochlore study, a non-zero (and positive) thermal Hall effect was measured in $\text{Tb}_2\text{Ti}_2\text{O}_7$, but a negligible κ_{xy} was detected in $\text{Y}_2\text{Ti}_2\text{O}_7$ (Fig. 1(b)). It was initially speculated that the thermal Hall signal in $\text{Tb}_2\text{Ti}_2\text{O}_7$ was due to some exotic spin excitations [17]. However, a subsequent study found that the κ_{xy} signal remains as strong when 70% of the magnetic Tb ions are replaced by non-magnetic Y ions, thereby dramatically altering the frustrated spin-liquid state of pure $\text{Tb}_2\text{Ti}_2\text{O}_7$ [18]. This led to the conclusion that phonons are in fact the heat carriers responsible for the thermal Hall effect in these pyrochlores. Moreover, the fact that κ_{xy} becomes negligible in $\text{Y}_2\text{Ti}_2\text{O}_7$, when all Tb is replaced by Y, indicates that magnetism plays a key role in the generation of the phonon thermal Hall effect in these pyrochlores.

Turning to our own study, we also observe a non-zero κ_{xy} in TmVO_4 , another oxide with magnetic ions (Tm), and we also attribute this Hall effect to phonons, as

argued above. In our comparison with $\text{Tb}_2\text{Ti}_2\text{O}_7$, we see two differences. The first is the fact that our non-magnetic parent compound, YVO_4 , also displays a non-zero κ_{xy} , unlike the negligible signal of $\text{Y}_2\text{Ti}_2\text{O}_7$. So in these vanadates, the phonon Hall effect does not depend crucially on the magnetic moment associated with Tm ions. Note that a non-zero thermal Hall effect from phonons has been observed in other non-magnetic insulators, such as strontium titanate [5] and black phosphorus [32].

The second difference is the sign of κ_{xy} : positive in $\text{Tb}_2\text{Ti}_2\text{O}_7$, negative in TmVO_4 . The sign of the phonon Hall conductivity is an entirely open question, on which existing theories shed little light. Phenomenologically, both signs are observed. For example, the phononic κ_{xy} is negative in SrTiO_3 [5], Cu_3TeO_6 [6] and black phosphorus [32], as well as in all cuprates, whether undoped [3, 4], hole-doped [2] or electron-doped [33]. A positive phononic κ_{xy} is observed in $\text{Fe}_2\text{Mo}_3\text{O}_8$ [1], $(\text{Tb}_{0.3}\text{Y}_{0.7})_2\text{Ti}_2\text{O}_7$ [18] and RuCl_3 [34, 35]. A remarkable feature of our findings is that κ_{xy} changes sign to positive upon introducing 30% Y into TmVO_4 (Fig. 5). This suggests that impurities (or defects), in much larger concentration in $\text{Tm}_{0.7}\text{Y}_{0.3}\text{VO}_4$ relative to either TmVO_4 or YVO_4 , is an important ingredient for the generation of a phonon thermal Hall effect.

It is instructive to look at the magnitude of κ_{xy} . As argued by others [1, 6, 32], the relevant quantity for this is the ratio κ_{xy}/κ_{xx} , namely the Hall angle. In Fig. 6, we see that in our three samples $|\kappa_{xy}/\kappa_{xx}| \simeq 1 \times 10^{-3}$ at $T = 20$ K and $H = 15$ T. This is quite typical. Indeed, the cuprate Mott insulators La_2CuO_4 , Nd_2CuO_4 and $\text{Sr}_2\text{CuO}_2\text{Cl}_2$ and the antiferromagnetic insulator Cu_3TeO_6 all have a Hall angle of about 3×10^{-3} at the same temperature and field [6]. The Kitaev spin liquid candidate RuCl_3 has a Hall angle of about 1×10^{-3} . Note that the magnitude of κ_{xy} varies by three orders of magnitude across those various materials.

It is worth noting that significantly larger thermal Hall angles have been observed in two cases so far: the Ce-doped cuprate Nd_2CuO_4 [33] and the Rh-doped iridate Sr_2IrO_4 [36]. In as-grown samples of Nd_2CuO_4 with 4% Ce and Sr_2IrO_4 with 5% Rh, $|\kappa_{xy}/\kappa_{xx}| \simeq 30 \times 10^{-3}$ at $T = 20$ K and $H = 15$ T. Both materials are insulators with antiferromagnetic order at these dopings, and it was argued in the latter study that impurities embedded in an antiferromagnetic environment strongly promote the phonon thermal Hall effect [36], as suggested theoretically for a mechanism of resonant side-jump scattering of phonons [16].

V. SUMMARY

We have measured a non-zero thermal Hall conductivity κ_{xy} in the vanadates TmVO_4 , YVO_4 and $\text{Tm}_{0.7}\text{Y}_{0.3}\text{VO}_4$. All evidence points to phonons as the heat carriers responsible for generating this Hall effect.

The magnitude of the Hall response is similar in all three, with a Hall angle of $|\kappa_{xy}/\kappa_{xx}| \simeq 1 \times 10^{-3}$ at $T = 20$ K and $H = 15$ T, comparable to the phonon Hall effect in several insulating materials. This shows that Tm ions do not play an essential role in generating the Hall effect in these rare-earth vanadates. While the sign of κ_{xy} in the two stoichiometric compounds TmVO_4 and YVO_4 is negative, we find a positive sign in the more disordered $\text{Tm}_{0.7}\text{Y}_{0.3}\text{VO}_4$. This points to a special role played by impurities in this family of materials.

ACKNOWLEDGMENTS

We thank S. Fortier for his assistance with the experiments. L. T. acknowledges support from the Canadian Institute for Advanced Research (CIFAR) as a CIFAR Fellow and funding from the Institut Quantique, the Natural Sciences and Engineering Research Council of Canada (NSERC; PIN:123817), the Fonds de Recherche du Québec - Nature et Technologies (FRQNT), the Canada Foundation for Innovation (CFI), and a Canada Research Chair. This research was undertaken thanks in part to funding from the Canada First Research Excellence Fund.

Crystal growth and characterization performed at Stanford University was supported by the Air Force Office of Scientific Research under award number FA9550-20-1-0252. MPZ was also partially supported by a National Science Foundation Graduate Research Fellowship under grant number DGE-1656518.

[1] T. Ideue, T. Kurumaji, S. Ishiwata, and Y. Tokura, Giant thermal hall effect in multiferroics, *Nature Materials* **16**, 797–802 (2017).

[2] G. Grissonnanche, A. Legros, S. Badoux, E. Lefrançois, V. Zatko, M. Lizaire, F. Laliberté, A. Gourgout, J.-S. Zhou, S. Pyon, T. Takayama, H. Takagi, S. Ono, N. Doiron-Leyraud, and L. Taillefer, Giant thermal hall conductivity in the pseudogap phase of cuprate superconductors, *Nature* **571**, 376–380 (2019).

[3] G. Grissonnanche, S. Thériault, A. Gourgout, M.-E. Boulanger, E. Lefrançois, A. Ataei, F. Laliberté, M. Dion, J.-S. Zhou, S. Pyon, T. Takayama, H. Takagi, S. Ono, N. Doiron-Leyraud, and L. Taillefer, Chiral phonons in the pseudogap phase of cuprates, *Nature Physics* **16**, 1108–1111 (2020).

[4] M.-E. Boulanger, G. Grissonnanche, S. Badoux, A. Allaire, E. Lefrançois, A. Legros, A. Gourgout, M. Dion, C. H. Wang, X. H. Chen, R. Liang, W. N. Hardy, D. A. Bonn, and L. Taillefer, Thermal hall conductivity in the cuprate mott insulators nd_2cu_4 and $\text{sr}_2\text{cu}_2\text{cl}_2$, *Nature Communications* **11**, 5325 (2020).

[5] X. Li, B. Fauqué, Z. Zhu, and K. Behnia, Phonon thermal hall effect in strontium titanate, *Phys. Rev. Lett.* **124**, 105901 (2020).

[6] L. Chen, M.-E. Boulanger, Z.-C. Wang, F. Tafti, and L. Taillefer, Large phonon thermal hall conductivity in the antiferromagnetic insulator $\text{cu}_{3}\text{sub}_3\text{teo}_3\text{sub}_6$, *Proceedings of the National Academy of Sciences* **119**, e2208016119 (2022).

[7] C. Strohm, G. L. J. A. Rikken, and P. Wyder, Phenomenological evidence for the phonon hall effect, *Phys. Rev. Lett.* **95**, 155901 (2005).

[8] M. Mori, A. Spencer-Smith, O. P. Sushkov, and S. Maekawa, Origin of the phonon hall effect in rare-earth garnets, *Phys. Rev. Lett.* **113**, 265901 (2014).

[9] T. Qin, J. Zhou, and J. Shi, Berry curvature and the phonon hall effect, *Phys. Rev. B* **86**, 104305 (2012).

[10] M. Ye, L. Savary, and L. Balents, Phonon hall viscosity in magnetic insulators, *arXiv [Preprint]* (2021), arXiv:2103.04223.

[11] Y. Zhang, Y. Teng, R. Samajdar, S. Sachdev, and M. S. Scheurer, Phonon hall viscosity from phonon-spinon interactions, *Phys. Rev. B* **104**, 035103 (2021).

[12] R. Samajdar, S. Chatterjee, S. Sachdev, and M. S. Scheurer, Thermal hall effect in square-lattice spin liquids: A schwinger boson mean-field study, *Phys. Rev. B* **99**, 165126 (2019).

[13] L. Mangeolle, L. Balents, and L. Savary, Phonon thermal hall conductivity from scattering with collective fluctuations, *Physical Review X* **12**, 041031 (2022).

[14] H. Guo and S. Sachdev, Extrinsic phonon thermal hall transport from hall viscosity, *Phys. Rev. B* **103**, 205115 (2021).

[15] X.-Q. Sun, J.-Y. Chen, and S. A. Kivelson, Large extrinsic phonon thermal hall effect from resonant scattering, *Phys. Rev. B* **106**, 144111 (2022).

[16] H. Guo, D. G. Joshi, and S. Sachdev, Resonant thermal hall effect of phonons coupled to dynamical defects, *Proceedings of the National Academy of Sciences* **119**, e2215141119 (2022).

[17] M. Hirschberger, J. W. Krizan, R. J. Cava, and N. P. Ong, Large thermal hall conductivity of neutral spin excitations in a frustrated quantum magnet, *Science* **348**, 106–109 (2015).

[18] Y. Hirokane, Y. Nii, Y. Tomioka, and Y. Onose, Phononic thermal hall effect in diluted terbium oxides, *Phys. Rev. B* **99**, 134419 (2019).

[19] Q. J. Li, Z. Y. Zhao, C. Fan, F. B. Zhang, H. D. Zhou, X. Zhao, and X. F. Sun, Phonon-glass-like behavior of magnetic origin in single-crystal $\text{tb}_2\text{ti}_{207}$, *Phys. Rev. B* **87**, 214408 (2013).

[20] I. Vinograd, K. R. Shirer, P. Massat, Z. Wang, T. Kissikov, D. Garcia, M. D. Bachmann, M. Horvatić, I. R. Fisher, and N. J. Curro, Second order zeeman interaction and ferroquadrupolar order in tmvo_4 , *NPJ Quantum Materials* **7**, 1–8 (2022).

- [21] Z. Wang, I. Vinograd, Z. Mei, P. Menegasso, D. Garcia, P. Massat, I. R. Fisher, and N. J. Curro, Anisotropic nematic fluctuations above the ferroquadrupolar transition in tmvo_4 , *Phys. Rev. B* **104**, 205137 (2021).
- [22] P. Massat, J. Wen, J. M. Jiang, A. T. Hristov, Y. Liu, R. W. Smaha, R. S. Feigelson, Y. S. Lee, R. M. Fernandes, and I. R. Fisher, Field-tuned ferroquadrupolar quantum phase transition in the insulator tmvo_4 , *Proceedings of the National Academy of Sciences* **119**, e2119942119 (2022).
- [23] Y.-H. Nian, I. Vinograd, T. Green, C. Chaffey, P. Massat, R. R. P. Singh, M. P. Zic, I. R. Fisher, and N. J. Curro, Spin-echo and quantum versus classical critical fluctuations in tmvo_4 , *arXiv [Preprint]* (2023), arXiv:2306.13244.
- [24] M. P. Zic, M. S. Ikeda, P. Massat, P. M. Hollister, L. Ye, E. W. Rosenberg, J. A. W. Straquadrine, B. J. Ramshaw, and I. R. Fisher, Giant elastocaloric effect at low temperatures in tmvo_4 and implications for cryogenic cooling, *arXiv [Preprint]* (2023), arXiv:2308.15577.
- [25] R. Feigelson, Flux Growth of Type RVO_4 Rare-Earth Vanadate Crystals, *Journal of the American Ceramic Society* **51**, 538–539 (1968).
- [26] S. H. Smith and B. M. Wanklyn, Flux growth of rare earth vanadates and phosphates, *Journal of Crystal Growth* **21**, 23–28 (1974).
- [27] H. Suzuki, T. Inoue, and T. Ohtsuka, Enhanced nuclear cooling and spin-lattice relaxation time in tmvo_4 and tmpo_4 , *Physica B+C* **107**, 563–564 (1981).
- [28] A. H. Cooke, S. J. Swithenby, and M. R. Wells, The properties of thulium vanadate — an example of molecular field behaviour, *Solid State Communications* **10**, 265–268 (1972).
- [29] B. Daudin and B. Salce, Thermal conductivity of rare earth vanadates and arsenates undergoing a cooperative jahn-teller effect, *Journal of Physics C: Solid State Physics* **15**, 463–475 (1982).
- [30] W. Mutscheller and M. Wagner, Thermal conductivity of cooperative jahn-teller e-systems, *Physica Status Solidi (b)* **134**, 39–52 (1986).
- [31] W. Mutscheller and M. Wagner, The influence of magnetic fields on the thermal conductivity of the cooperative vibronic system tmvo_4 , *Physica Status Solidi (b)* **144**, 507–518 (1987).
- [32] X. Li, Y. Machida, A. Subedi, Z. Zhu, L. Li, and K. Behnia, The phonon thermal hall angle in black phosphorus, *Nature Communications* **14**, 1027 (2023).
- [33] M.-E. Boulanger, G. Grissonnanche, E. Lefrançois, A. Gourgout, K.-J. Xu, Z.-X. Shen, R. L. Greene, and L. Taillefer, Thermal hall conductivity of electron-doped cuprates, *Phys. Rev. B* **105**, 115101 (2022).
- [34] E. Lefrançois, G. Grissonnanche, J. Baglo, P. Lampen-Kelley, J.-Q. Yan, C. Balz, D. Mandrus, S. E. Nagler, S. Kim, Y.-J. Kim, N. Doiron-Leyraud, and L. Taillefer, Evidence of a phonon hall effect in the kitaev spin liquid candidate $\alpha\text{-rucl}_3$, *Phys. Rev. X* **12**, 021025 (2022).
- [35] R. Henrich, M. Roslova, A. Isaeva, T. Doert, W. Brenig, B. Büchner, and C. Hess, Large thermal hall effect in $\alpha\text{-rucl}_3$: Evidence for heat transport by kitaev-heisenberg paramagnons, *Phys. Rev. B* **99**, 085136 (2019).
- [36] A. Ataei, G. Grissonnanche, M.-E. Boulanger, L. Chen, E. Lefrançois, V. Brouet, and L. Taillefer, Impurity-induced phonon thermal hall effect in the antiferromagnetic phase of sr_2iro_4 , *arXiv [Preprint]* (2023), 2302.03796.